Real-Time Approaches for Characterization of Fully and Partially Scanned Canopies in Groves

Fernando A. Auat Cheein[1], José Guivant[2], Ricardo Sanz[3],
Alexandre Escolà[3], Francisco Yandún[1], Miguel Torres-Torriti[4], Joan R Rosell-Polo[3*]
[1]Department of Electronic Engineering, Universidad Técnica Federico Santa María, Valparaíso, Chile
[2]School of Mechanical Engineering, University of New South Wales, Australia
[3]Research Group on AgroICT & Precision Agriculture, Department of Agricultural and Forest Engineering, Universitat de Lleida- Agrotecnio Center, Lleida, Spain
[4]Pontificia Universidad Católica de Chile, Santiago, Chile.

[*]Joan R. Rosell-Polo, jr.rosell@eagrof.udl.cat
Av. Rovira Roure 191, 25198 Lleida, Spain
Phone: +34 973 702861

Abstract- Efficient information management in orchard characterization leads to more efficient agricultural processes. In this brief, a set of computational geometry methods are presented and evaluated for orchard characterization; in particular, for the estimation of canopy volume and shape in groves and orchards using a LiDAR (Light Detection And Ranging) sensor mounted on an agricultural service unit. The proposed approaches were evaluated and validated in the field, showing they are convergent in the estimation process and that they are able to estimate the crown volume for fully scanned canopies in real time; for partially observed tree crowns, accuracy decreases up to 30% (the worst case). The latter is the major contribution of this brief since it implies that the automated service unit does not need to cover all alley-ways for an accurate modeling of the orchard, thus saving valuable resources.

Keywords: Crown volume; LiDAR sensor; Mobile terrestrial laser scanner; agricultural robotics.

1. Introduction

In agriculture, knowledge of the characteristics of plants is essential to perform an efficient and effective management of crops. In recent years, the availability of affordable sensors and electronic systems capable of facilitating the performance of intensive measurements has gradually replaced traditional methods based on manual measurements. At present, there is hardly any relevant plant characteristic without an associated sensory system based on the use of electronics for its determination. As a result, i) the accuracy of the measurements has drastically increased, ii) data acquisition has been eased, lightened and, in many cases, automated, iii) the traditional analysis of a reduced number of manually-collected data has given way to the

processing of files with huge amounts of data resulting from the measurements provided by the sensors and iv) decision making in crop management can be supported by information now available and impossible to have in the past. Among the characteristics of crops, geometry deserves special mention (canopy height, width and volume) as well as structural parameters (leaf area index, canopy porosity and permeability and wood structure) due to their great influence on the behavior of plants interacting with solar radiation, water and nutrients at their disposal (Lee and Ehsani, 2009) as well as on the knowledge and prediction of the vigor and quality of the produced crop (Arnó et al., 2013). These parameters also have a key role in assessing the efficiency and effectiveness of the main operations performed in the orchards, such as the application of inputs (fertilizers, irrigation and plant protection products against pests and diseases), pruning and harvesting (Sanz et al., 2011; Rosell and Sanz, 2012). Several studies have shown the existence of a relationship between the geometrical parameters of a crop and yield (Pascual et al., 2011).

Among the geometric parameters of plants, canopy volume has a special significance because it combines, in a single variable, the width, the height, the geometric shape and the structure of trees (Sanz et al., 2013). For this reason, its determination in a reliable, systematic and affordable way, both in cost and time, is a priority in the present and near future of Precision Agriculture/Fructiculture defined as the one that takes full advantage of the ICT (Information and Communications Technology) systems, geostatistics and decision making support systems.

Usually, precise measurement of the volume of a canopy requires of costly man-made measurements on the plants with the corresponding time and economical cost. However, several

63 sensor-based approaches have been published in the scientific literature that deal with the
64 problem of estimating the volume of canopies. The most used techniques to determine the
65 canopy volumes are based either on the use of electromagnetic radiation, mainly in the spectrum
66 range from the ultraviolet to the infrared, including the visible, or on the use of ultrasonic waves.
67 The most widespread systems in the first group are those based on the use of digital
68 photography, photogrammetry, and stereoscopy techniques as well as LiDAR (Light Detection
69 and Ranging) sensors (Rosell and Sanz, 2012). Indeed, the latter is increasingly being used in
70 agricultural applications due to its high accuracy, reading speed rates and versatility. A LiDAR
71 sensor estimates the distance apart of the object of interest, using -in some technologies- the
72 Time of Flight (ToF) principle (Newnham et al., 2012). In practice most used LiDAR scanners
73 perform sweeps in a plane (2D) or in the space (3D) by modifying the direction at which the
74 laser beam is emitted. A very common configuration in agricultural research applications is what
75 is known as mobile terrestrial laser scanner (MTLS), a 2D LiDAR sensor mounted on a vehicle
76 moving along the alley-ways between rows of trees in an orchard in order to obtain the scanning
77 of the entire crop in 3D, (Rosell et al., 2009a, 2009b). This operation mode usually requires a
78 high precision GNSS receiver to know the spatial coordinates of the LiDAR sensor at all times.
79 In this context Pforte et al. (2012) show a LiDAR system combined with a monocular vision
80 system used to estimate the plum tree canopy cover, using a LiDAR sensor mounted on a tractor.
81 The machinery drives through the alleys while the LiDAR, strategically located above the
82 canopies, acquires the range information. One of the main drawbacks of the system is the height
83 of the trees: they cannot be taller than the tractor, as it is presented in (Pforte et al., 2012). In
84 (Keightley and Bawden, 2010) a LiDAR sensor mounted on a ground tripod is used for 3D
85 volumetric modeling of a grapevine. The system does not consider position errors (as mentioned

in Auat Cheein and Guivant, 2014) and the validation was performed under laboratory conditions. In (Bucksch and Fleck, 2009; Raumonen et al., 2013) a ground fixed LiDAR sensor is used to 3D model the tree skeletons, based on a graph splitting procedure to extract branches from the cloud of points. Although the system efficiently extracts the skeleton patterns from several trees, it does not offer a real time solution and its robustness to leaves density is not provided in the research. In the same line, Cote et al. (2009), explores and tests the use of LiDAR scanners in tree modeling. In addition, Moorthy et al. (2007) used a 3D LiDAR to measure structural and biophysical information of individual trees. Although a consistent statistical analysis is presented regarding the estimation of leaf area (unlike Beland et al. (2011) and Hosoi and Omasa (2006)), no information is provided regarding the geometric determination of the treetop. Fieber et al. (2013) used a LiDAR to classify ground, trees and oranges using only the reflected waveforms from the LiDAR, avoiding the need of using geometric information. Although efficient, the proposal was not tested for real time implementations but for batch processing only. In addition, no information is provided regarding shapes or sizes of the agricultural features. In Walklate et al. (2002) a LiDAR sensor and a GPS receiver are mounted on a same chassis for 3D reconstruction of orchards. No information is provided regarding the geometric processing. Instead, the research is focused on using the 3D information for spray management. The performance of the previous methods relies on the precision of the GPS (see Auat Cheein and Guivant, 2014). Méndez et al. (2014, 2013) used a LiDAR for skeleton reconstruction of a grove and for vegetative measures. On the other hand, Jaeger-Hansen et al. (2012) uses a similar hardware and provides a first estimate of the treetop surface using ellipses and minimum square fitting techniques. In addition, in (Rosell et al., 2009b), a first study in 3D orchard reconstruction is presented, in which a LiDAR and a differential GPS are used for

mapping the environment. Although based on manual fitting techniques, the authors provided a first approach for groves characterization.

The huge amount of data generated by electronic measuring systems such as MTLS makes it a must the development of both i) hardware fast enough and with enough storage capacity, as well as ii) efficient software capable of processing such large data sets, in many cases being able to process them as quickly as possible to allow for real time crop management applications. With regards to MTLS, the results obtained from the measurements are point clouds (though georeferenced using GNSS receiver) which, in the case of an entire row or orchard, can contain tens of millions of points, each one with information on their geographical coordinates and, in some cases, additional information such as reflectance and color. In the presence of such huge amount of information it is essential to perform the extraction of the parameters of interest, such as the volume of plants, by means of automated algorithms with low computational time cost. An alternative to lighten the volume of data to be measured and processed and thus facilitate real-time operation consists of measuring the tree rows from one side only. In this way, the monitoring of the entire tree crop can be done with half the time by passing the MTLS measuring system along alternated rows. Arnó et al. (2013) showed the advantages of scanning a vineyard from only one side of the rows when estimating the LAI with an MTLS. Additionally, it was also concluded that, in the N-S oriented vineyards analyzed, the estimation of LAI was to a great extent independent of which side of the row was scanned (Arnó et al., 2015). In the specific case of the determination of the volume of the crowns, it must be verified that the results obtained by measuring alternated rows are sufficiently accurate and reliable before giving this proposal as valid.

In the field of Precision Agriculture/Fructiculture, the acquired information should be reliable for agricultural purposes constrained to minimize available resources. The latter is the main issue faced in this work: the characterization of orchards when are partially and fully scanned by a LiDAR. We propose and evaluate the performance of several methodologies developed for this aim.

In this work we implement four methodologies based on LiDAR readings for characterization of canopies: a convex hull approach, a segmented convex hull approach, a cylinder based approach and an occupancy grid approach. Such methodologies use the advantages of computational geometry to obtain an estimate of the canopy volume, considering that the canopy's true volume is unknown. The methodologies, based only on LiDAR range readings (thus no attenuation of the beam is considered) are evaluated, compared among each other and validated with real data. Taking into consideration that one of the challenges is to reduce the resources consumption of the service unit, the canopy characterization procedures are also applied when canopies are partially scanned, thus avoiding the need of visiting all the alley-ways in the grove. The four computational methodologies shown in this work provide the geometry associated with the canopy, which can be used later for spray management and other operations performed in the orchards.

2. Materials and Methods

In this work, four computational approaches are presented for canopy characterization of orchards and groves: i) a convex hull approach, ii) a segmented convex hull approach, iii) a

155 cylinder-based modeling of canopies and iv) a 3D occupancy grid approach (Hosoi et al., 2006).
156 The four methods are first evaluated using a known template and then they are tested in the field.
157 For the programming of the approaches, we have used Matlab2013 environment running under
158 Windows 8 operative system.
159
160 **2.1 Test with a simulated point cloud template**
161 The four methods were first compared using a simulated point cloud template shown in Fig. 1.
162 The template consisted of a non-convex body with a known volume (see Fig. 1.a). A uniform
163 random point cloud was sparsely spread within the rigid body, as shown in Fig. 1.b. For the
164 analysis presented herein, a non-convex body characterization was chosen instead of a convex
165 one since convex geometries could lead to trivial characterizations (especially when using
166 convex hull approaches), as previously published by the authors in (Auat Cheein and Guivant,
167 2014). The volume of the rigid body shown in Fig. 1.a is approximately 6.28 m^3. In this work we
168 used point clouds for orchard characterization since, as explained later, the experimental setup
169 consisted of a 2D LiDAR sensor (which acquires range measurements) mounted on an
170 automated service unit used for agricultural monitoring.
171
172
173
174

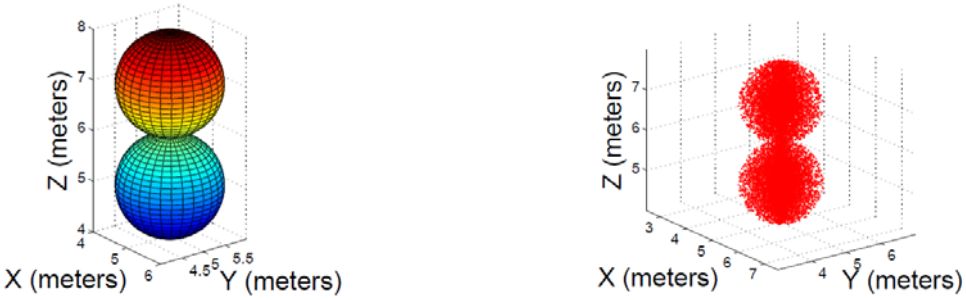

1.a 1.b

Figure 1- Non-convex point cloud template. Figure 1.a shows the rigid body used as a template for testing the proposed methodologies for orchard characterization, whereas Fig. 1.b shows the points cloud with 10000 points, belonging to the rigid body.

2.1.1 Convex hull approach

The convex hull approach is based on a previous work of the authors (Auat Cheein and Guivant, 2014). The approach is based on finding the points (from the provided cloud of points) that belong to the closest convex set that contains all the points from such a cloud. The main features of this technique can be summarized as follows:

- The convex hull can be optimized for real-time implementations (Auat Cheein and Guivant, 2014).
- It finds the smallest convex set that contains the entire cloud of points. The points of the convex hull set can be seen as the corners of a rigid body that contains the cloud of points and a volume can be associated to it. In fact, the convex hull approach provides of an upper bound for treetop volume estimation, as shown in (Auat Cheein and Guivant, 2014), and the references therein.

- As the number of points in the cloud tends to infinity, the volume of the convex hull set associated with such cloud tends to its minimum.

Further and more detailed information regarding the convex hull approach and its implementation in treetop volume estimation can be found in (Auat Cheein and Guivant, 2014).

2.1.2 Segmented Convex hull approach

We implemented a segmented convex hull approach, that takes into account the advantages of the convex hull algorithm shown in Section 2.1 (and in (Auat Cheein and Guivant, 2014)) but restricted to a portion of the cloud of points, thus overcoming the overestimation problem of the first approach. Briefly,

- Let Ω be the point cloud to be analyzed, and z_{min} and z_{max} the minimum and maximum values, respectively, of the z-coordinates of the points from Ω.
- Let δ be a step criterion in such a way that $z_{max} - z_{min} = n \times \delta$ where n is a positive integer.
- Then, we calculate the convex hull associated with each segment from Ω: $\forall\, p \in \Omega: z_{min} \times n \times \delta \leq p_z < z_{max} \times (n+1) \times \delta$, with $n = 0, 1, \ldots, \frac{z_{max} - z_{min}}{\delta}$ and p_z stands for the z-coordinate of any point $p \in \Omega$. Thus, we divide Ω into sets of wide δ in the z-coordinate, and calculate their corresponding convex hull.
- The final volume is estimated by adding all the partial volumes associated with each segment.

215 2.1.3 Cylinder-based Modeling approach

216 The cylinder-based approach is based on the fact that several treetops (from commercial
217 intensive groves) show some symmetry on their morphology. Such is the case shown in Fig. 2
218 (corresponding to an olive grove). Apple, lemon, peach and avocado trees (all main fruit tree
219 crops in Chile) also have symmetry on their crowns.

220

221

222 **Figure 2-** Experimental olive grove.

223

224 The cylinder-based approach uses the symmetry of the canopy as a hypothesis. Briefly,

225 - As in the previous method, let Ω be the point cloud to be characterized, and z_{min} and
226 z_{max} the minimum and maximum values of the z-coordinates of the points from Ω.
227 - Let δ be a step criterion in such a way that $z_{max} - z_{min} = n \times \delta,$ where n is a
228 positive integer.
229 - Let $\Omega_{\delta,i}$be the set of points from Ω such that: $i \times \delta + z_{min} \leq p_z < (i+1) \times \delta + z_{min}$,
230 where $p_z$is the z-coordinate of all points from Ω and $i = 0 \ldots n-1$. Thus, as in the
231 previous method, we divided the Ω into segments over the z-axis.

- For each segment, we calculate its center of mass. Such center of mass becomes the center of the cylinder. Its radius is the longest distance from the center of mass to any point from $\Omega_{\delta,i}$.

As it can be seen, as in the previous method, the selection of δ is a designer criterion. In this work, we set δ to 0.2 meters.

2.1.4 3D Occupancy Grid approach

Occupancy grid approaches are commonly used in 2D and 3D robotic mapping. In this case, we used 3D occupancy gridding for clustering the point cloud obtained from the scanned canopy. Briefly, as in the previous methods, let Ω be the point cloud to be processed; let δ be the length of the edge of a cube; for all the points in Ω, we applied the gridding approach presented in (Choset et al., 2005) in which each cell is a cube of size δ^3. All cells are disjoint between each other. The total volume of Ω is estimated by adding the volume of all the generated cubes.

2.1.5 Performance comparison

When implementing computational algorithms applied to real time processing of data, their computational performance represents a decision criterion at the moment of choosing the best approach. In this context, the performance of the algorithms can be described in the following manner:

1. The *computational cost*. It is associated with the computational resources demanded by the system for data processing.

2. The *accuracy*. The approaches shown here build 3D models of the treetops. The accuracy is related to how representative the models are with respect to the actual object (the tree crown). In this work, we seek to estimate the volume of the canopy. Therefore, the accuracy of the approaches proposed is intrinsically related to how accurate the canopy volume estimation is.
3. The *convergence*. As it will be shown, some techniques approach the steady state canopy volume estimation faster than others (with less data). Therefore, the convergence is intrinsically related with the amount of data needed to reliably estimate a volume.

2.2 Test with point clouds from real orchards

2.2.1 Field measurements description

The four methods were subsequently evaluated with point clouds obtained from real fruit trees orchards. The measuring methodology employed in this work has been developed, tested and previously published by the authors in (Rosell et al., 2009a, 2009b; Sanz et al, 2011, 2013). Briefly: the orchards used in the test were arranged in rows of *Blanquilla* pear trees, forming a continuous wall of vegetation. A mobile terrestrial laser scanning system using a SICK LMS200 LiDAR sensor was developed for that study. The LiDAR sensor is able to scan in 2D (one single plane), from 0 to 180 degrees and with a maximum range of 8 m. The LiDAR sensor was mounted vertically (as shown in Fig. 3) in order to obtain proper vertical slides of the canopy cross-section profiles as the vehicle navigates the environment. The sensor provides with the distance value obtained from the first echo and the intensity of that returned beam with no chance to analyze the full returning signal.

277 Details of the experimental set-up and further information regarding the agricultural environment
278 and the data set used in this work can be found in (Sanz et al., 2011, 2013).

279

280 **Figure 3-** Two views of the developed scanning system based on the SICK LiDAR.

281

282 The field data was acquired using a laptop computer. The point cloud matching process was
283 achieved using characteristic features previously located in the environment (Sanz et al., 2013).
284 Figure 4 shows a 3D reconstruction of the environment, using Cloud Compare software
285 (available at http://www.danielgm.net/cc/). In particular, Fig. 4 shows different views of the
286 orchard, as the scanning system was navigating through it. It is to be noted that data depicted in
287 Fig. 4 suffer from lack of processing; thus, rough data is shown. In order to obtain the 3D
288 reconstruction of the environment, we have followed the guidelines shown in (Rosell et al.,
289 2009a, 2009b) to properly build the navigated orchard. In order to obtain the point cloud shown
290 in Fig. 4, the developed scanning system first had to map its left side and then its right side, as
291 shown in Fig. 5. As it can be seen, the distance between two consecutive stems is approximately
292 2 m, and the length of the system vehicle/scanner (shown in Fig. 3) is approximately 4 m.
293 Features labeled as *doors*, correspond to artificial structures manually located in the grove to be

294 used for improving correspondence in data matching processes. Additional details can be found
295 in (Sanz et al., 2011, 2013).
296

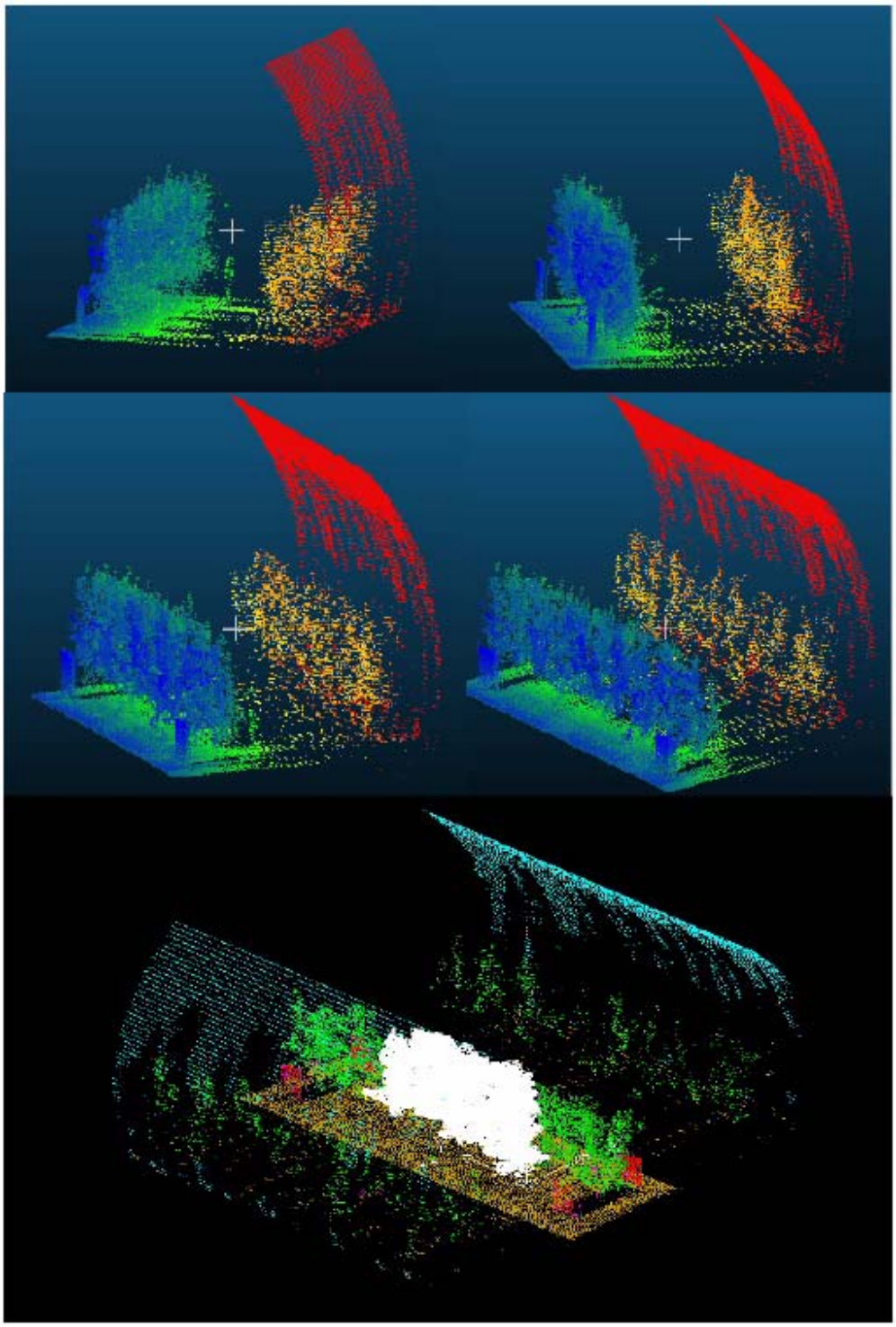

Figure 4- Reconstruction of the 3D point cloud obtained with the scanning system shown in Fig. 3.

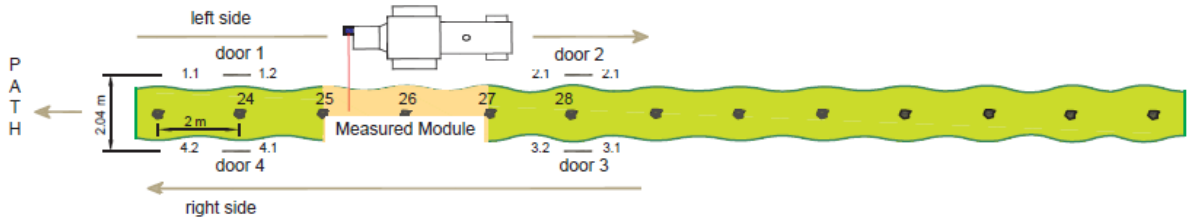

Figure 5- Navigation of the scanning system through the orchard.

2.2.2 Application to the scanned canopy

The data set used in this work corresponds to the point cloud shown in Fig. 4, following the vehicle navigation shown in Fig. 5, i.e. the system first scanned the row from one side and then from the other side. The measurements were located in a global coordinate frame using point cloud matching techniques, as previously presented in (Sanz et al., 2013). Briefly,

1. The LiDAR sensor works synchronously acquiring 3D information from the environment. It is to be mentioned that consistency of the 3D reconstruction stage was not addressed in this work.
2. The four approaches for estimating the canopy volume presented in this work (the convex hull, the segmented convex hull, the cylinder-based modeling and the 3D occupancy gridding approach) are able to process batch of 3D data. Therefore, if we collect 3D data from the entire orchard or just from a particular tree, the algorithms will obtain their corresponding estimations. However, since not only the volume of a treetop is important, but also its geometry and density, among others, we have segmented the batch processing stage: the system collects data for 2 meters of motion of the scanner (which corresponds to the distance between two consecutive stems, as shown in Fig. 5). However, other approaches can also be applied at this stage.

3. Once collected, the 3D data are processed. First, using Cartesian clustering algorithms (as the ones shown in (Mella et al., 2014)), the points associated with the ground are rejected. In addition, only the points associated with the closer row are processed (thus, points at a distance further than 3 meters, are rejected. This is possible since the alley-ways width is approximately 2.5 meters).
4. For each batch of 3D data, the volume is estimated and stored in the system.

In this work, the data used corresponds to the inner row of orchards (white colored in Fig. 4).

3. Results and discussion

3.1 Results from a simulated point cloud template

3.1.1 Convex hull approach

Figure 6 shows three examples of convex hull for different number (N) of points (N = 100, N = 1000 and N = 10000). As it can be seen, as the number of points increases, the convex hull better resembles the rigid body shown in Fig. 1.a, without its non-convex parts.

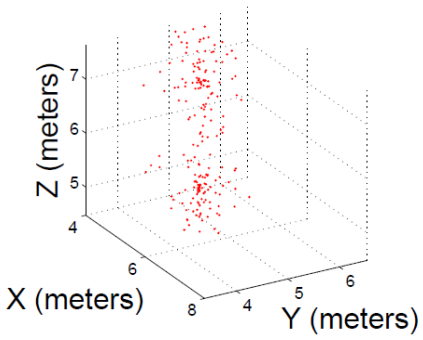

6.a

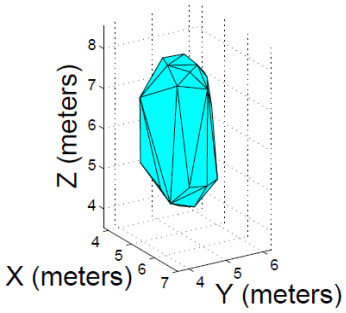

6.b

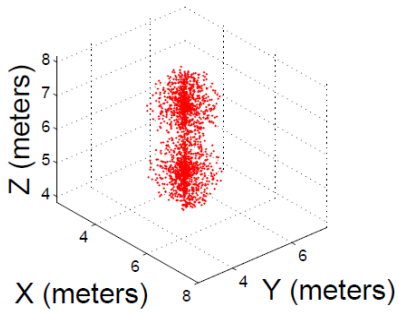

6.c

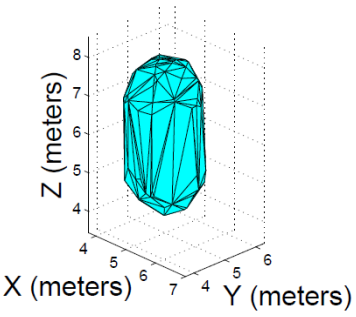

6.d

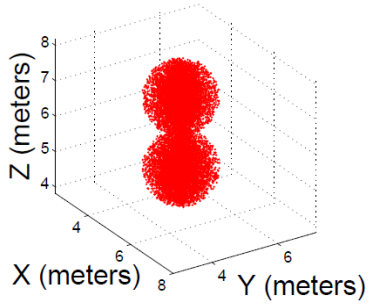

6.e

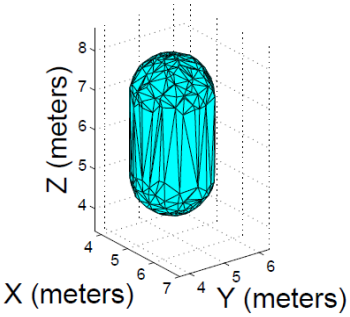

6.f

Figure 6- Convex hull examples. Figure 6.a shows a point cloud with N = 100 (number of points) according to the template shown in Fig. 1, whereas Fig. 6.b, shows its corresponding convex-hull. Figures 6.c-6.e show the point clouds for N = 1000 and N = 10000, with their corresponding convex-hull (Figs. 6.d-6.f).

One of the main drawbacks of the previous method can be seen in Fig. 6.f. The convex hull approach (when using the entire points cloud) filters the non-convex regions of the cloud, which leads to an overestimation of the volume associated with the point cloud. For example, as mentioned above, the volume of the template is approximately 6.28 m^3, whereas the volume calculated for Fig. 6.f is 9.87 m^3, clearly higher.

3.1.2 Segmented Convex-Hull approach

Fig. 7 shows the results of the segmented convex hull approach for N = 100, N = 1000 and N = 10000 (number of points in the cloud), where $\delta$was empirically determined as $\delta = 0.2$ meters.

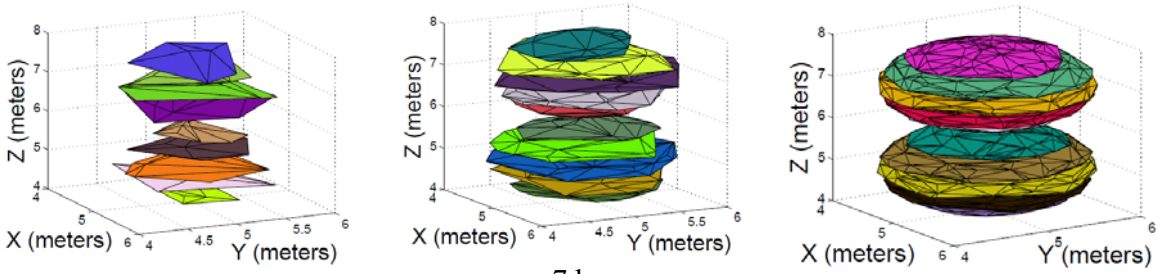

7.a 7.b 7.c

Figure 7- Segmented convex hull approach. Figure 7.a shows the case for N = 100, whereas Figs. 7.b and 7.c, show the results for N = 1000 and N = 10000 respectively.

In the results shown in Fig. 7, specifically, for N = 10000 (Fig. 7.c), the estimated volume was 7.24 m^3, only a 15% greater than the true volume of the template (6.28 m^3) and a 42% more accurate than the convex hull approach described in Section 2.1. Clearly, the segmented convex

363 hull approach outperforms the estimation of the single convex hull algorithm. In fact, the model
364 obtained in Fig. 7.c better resembles the point cloud of the template, shown in Fig. 1.
365 Additionally, the results depend on δ and on the number of points in the cloud. The higher the
366 number of points, the better the characterization of the canopy, as shown in (Auat Cheein and
367 Guivant, 2014; Rosell et al., 2009a, 2009b); and δ should be chosen in such a way that represents
368 the orchard (a smaller δ could lead to empty sets of points; on the other hand, a greater δ could
369 lead to an amorphous characterization). In Section 2.5 we provide a deeper analysis of
370 performance of each of the methods proposed in this work.
371
372 3.1.3 Cylinder-based Modeling approach
373 Figure 8 shows three examples of the cylinder-based approach for the template shown in Fig. 1,
374 for N = 100, N = 1000 and N = 10000, as in the previous cases.
375

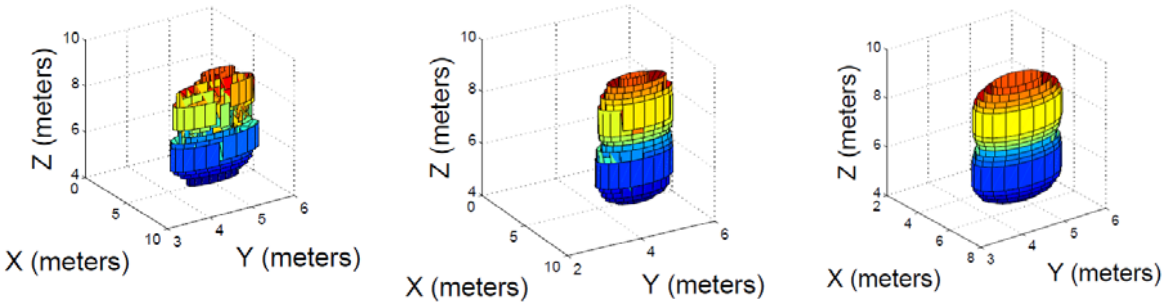

376
377 **Figure 8-** Cylinder-based modeling. Figure 8.a shows the case for N = 100, whereas Figs. 8.b
378 and 8.c show the case for N = 1000 and N = 10000 respectively.
379

For the case shown in Fig. 8, for N = 10000, the estimated volume of the points cloud template is 7.27 m^3, which is very similar to the one obtained for the segmented convex hull approach. Further analysis regarding the estimation process is presented in Section 2.5. As it can be seen in Fig 8, as the number of points from the cloud increases, the cylinder based model better resembles the template.

3.1.4 3D Occupancy Grid approach

Fig. 9 shows two cases: for $\delta = 0.2$ meters and for $\delta = 0.4$ meters, with N = 100 (number of points). Clearly, δ is a designer criterion and represents a compromise between accuracy and performance, as will be shown later.

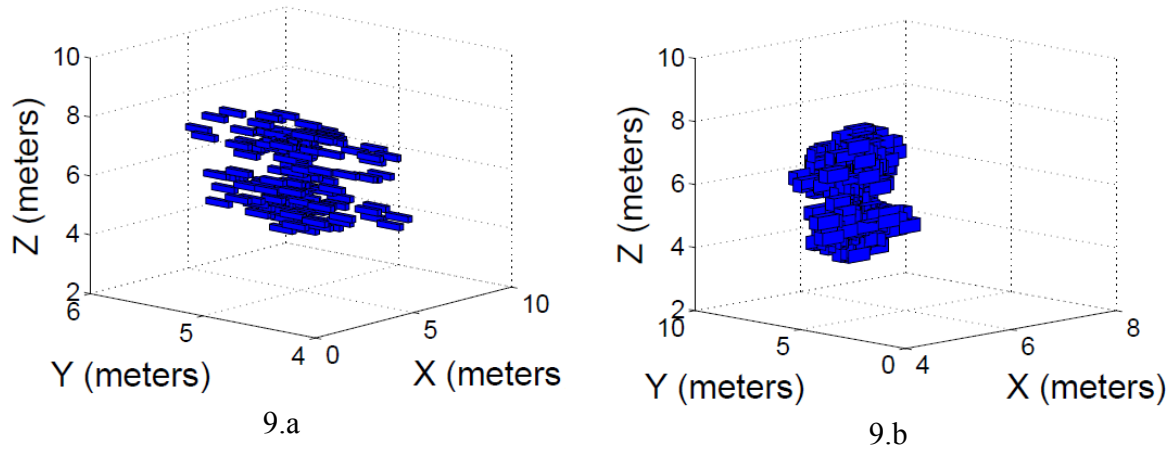

9.a 9.b

Figure 9- 3D occupancy grid with different size of cells. Figure 9.a shows the case for cells with $\delta = 0.2$ meters of edge's length; whereas Fig. 9.b shows the case for $\delta = 0.4$ meters.

In addition, Fig. 10 shows how the estimation evolves as the number of points of the cloud increases (N = 100, N = 1000 and N = 10000). For the cases shown in Fig. 10, δ was set to 0.2 meters.

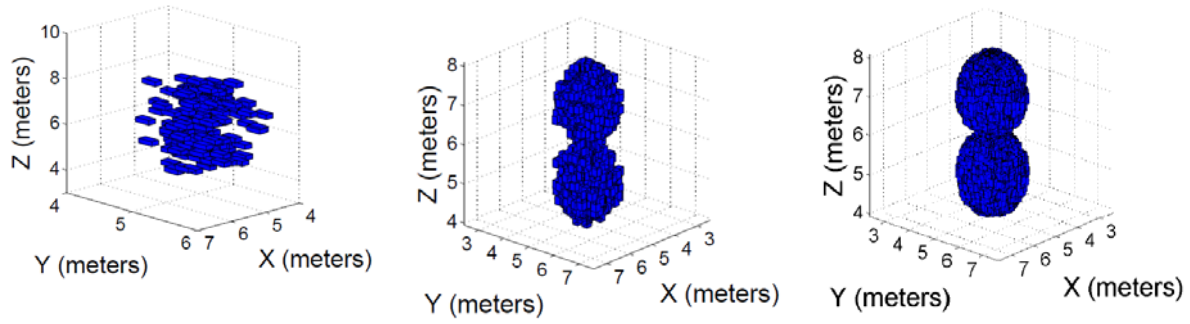

10.a 10.b 10.c

Figure 10- Occupancy grids for different number of points. Figure 10.a shows the case when N = 100; Fig. 10.b shows the case for N = 1000 and Fig. 10.c for N = 10000. The size of cubes remains the same ($\delta = 0.2$ meters).

It is interesting to note that, as N increases, the volume estimated by the occupancy grid method approaches the actual volume value of the template. For the case shown in Fig. 10, the estimated volume was 0.4 m^3 (for N = 100), 5.5 m^3 (for N = 1000) and 6.33 m^3 (for N = 10000), which is very close to the actual volume of the template shown in Fig. 1.a (i.e., 6.28 m^3). As it can be seen in Fig. 10, as N increases, the occupancy grid tends to the original template.

3.1.5 Performance comparison

Figure 11 shows the performance (from a computational cost, accuracy and convergence perspective) of the four approaches for canopy volume estimation proposed in this work, for the template used in Section 2. Figure 11.a shows the volume estimation for different number of points in the cloud. The dashed dark line represents the true volume of the template. Figure 11.b shows the computational cost (in seconds) required by the approaches to estimate the treetop volume according to different number of points; whereas Fig. 11.c shows how the gradient behaves for the four approaches. It is worth mentioning that the gradient of the curve represents the speed of the convergence process. As it can be seen, the gradients tend to zero, but at different rates.

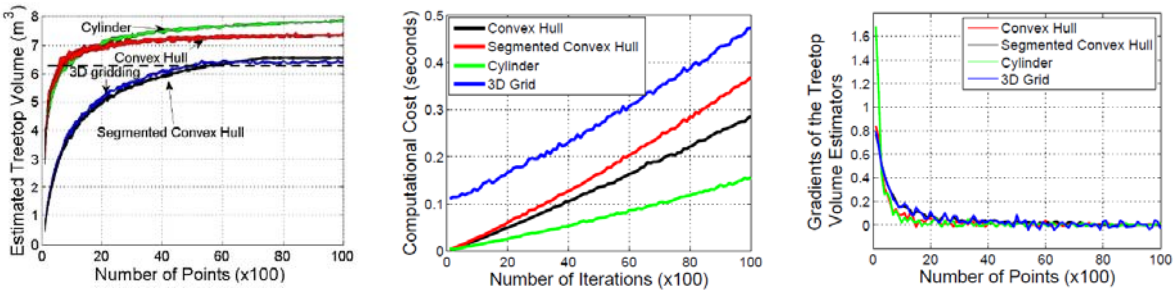

11.a 11.b 11.c

Figure 11- Performance analysis of the four treetop volume estimation approaches. Figure 11.a shows the behavior of the estimation as function of the number of points in the point cloud associated with the template; Fig. 11.b shows the computational cost (in seconds) of each approach according to the number of points of the cloud; and Fig. 11.c, shows the gradient behavior (obtained from Fig. 11.a).

As it can be seen, both the 3D occupancy grids and the segmented convex hull approaches show the best results in terms of accuracy of the estimation (as shown in Fig. 11.a). With 6000 points both approaches are able to estimate the volume of the template with an error of approximately 5%. As expected, the cylinder-based approach and the convex hull approach offer upper bounds of the volume estimation. The latter also affects the computational cost: since the convex hull approach and the cylinder-based approach over-estimate the treetop volume by neglecting non-convex regions of the cloud, their computational cost is lower than the ones shown by the segmented convex hull approach and the 3D grid. In addition, as shown in the gradients in Fig. 11.c, the convex hull and the cylinder-based approaches reach their steady state estimation faster than the other two approaches.

3.2 Results from real orchards

3.2.1 Fully observed canopies

The white colored portion shown in Fig. 4 corresponds to the inner 3D data batch shown in Fig. 12. Therefore, it is possible to see that according to the convex hull method (Fig. 12.a), the estimated volume is 17.47 m^3; according to the segmented convex hull, the estimated volume is 10.08 m^3; the cylinder based modeling approach estimates the volume in 28.40 m^3. Finally, the 3D occupancy grid approach estimation is 12.48m^3(with $\delta = 0.2$ m).

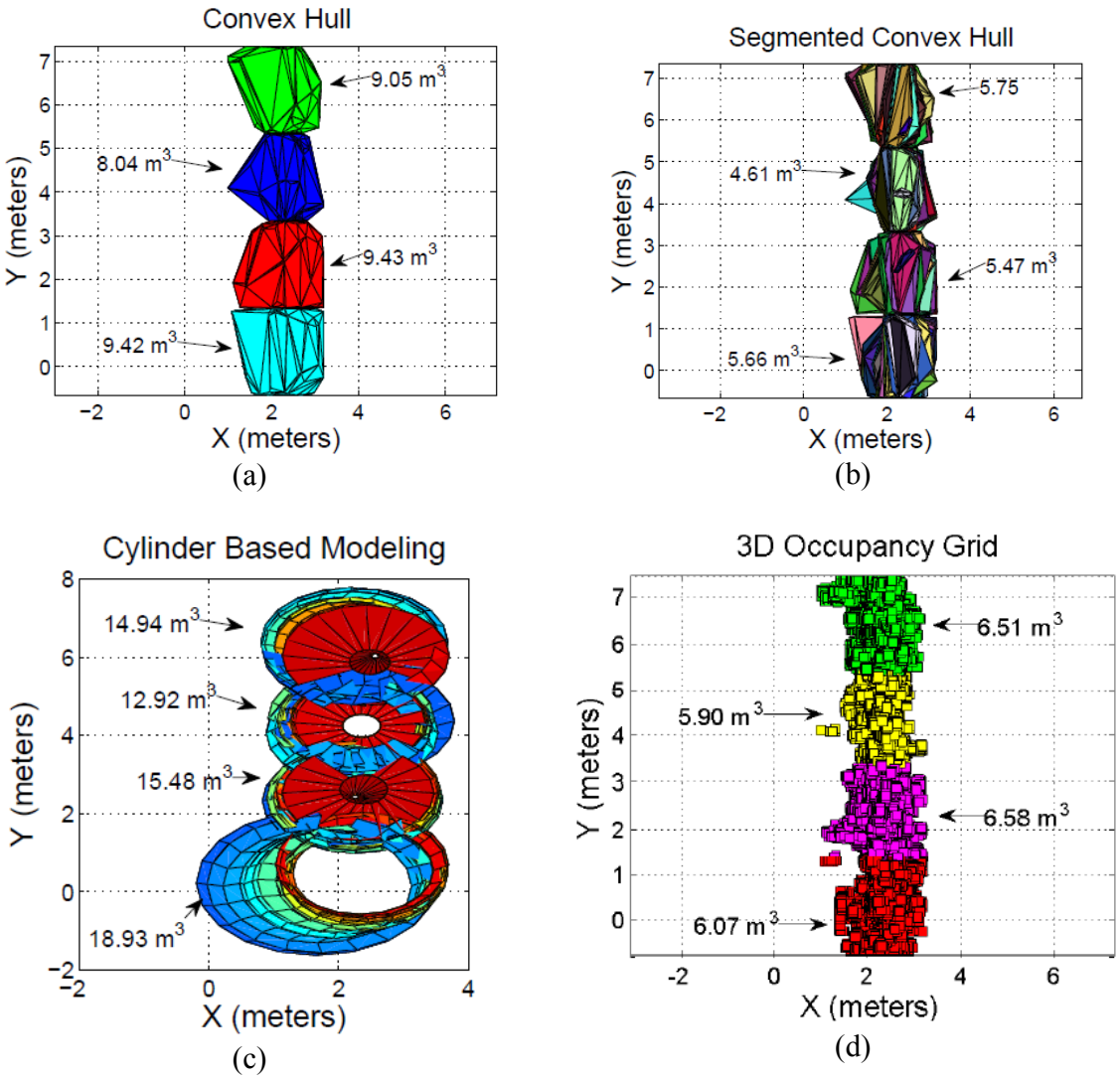

Figure 12- Volume estimation of a fully observed canopy. Figures 12.a-12.d show the four methodologies for estimating the row section canopy volume shown in Fig. 4.

In Fig. 12, it is clear that the cylinder-based modeling approach offers the highest volume estimation values when compared with the other approaches, for the same data batch. In addition, both the cylinder-based modeling and the convex hull approach offer convex modeling of the row. However, one single point separated from the cloud can produce differences of

458 several orders of magnitude in the estimation process. For example, see the first 3D batch of
459 data, shown in Fig. 12 (located at the bottom of the row view). For the cylinder-based modeling,
460 the estimated volume is almost twice the estimated volume by the convex hull approach.
461
462 In the same context, the segmented convex hull approach has similar estimation results than the
463 3D occupancy grid for all the 3D batches of data. It is to be noted that the 3D occupancy grid
464 offers a more refined estimation, as previously shown in Fig. 11. However, such resolution is one
465 of the main drawbacks of this technique as will be shown in the following section.
466
467 3.2.2 Partially observed canopies
468 Fig. 13 shows the orchard characterization using only the 3D batch data acquired from the right
469 side of the row (i.e. the first navigation of the scanning system). As in the fully observed canopy
470 case, we will evaluate the white colored region of the orchard, shown in Fig. 4. For the convex
471 hull approach, the estimated volume was 15.47 m^3; for the segmented convex hull approach,
472 7.26 m^3; for the cylinder based modeling, 16.73 m^3; whereas for the 3D occupancy grid
473 approach, 8.84 m^3. The results obtained here are of the same order of magnitude than the ones
474 obtained in the previous section. In average, and for the case study presented in this work, the
475 volume of partially observed canopies is estimated with up to 75% of correspondence, when
476 compared with the fully observable case. Table 1 shows a more detailed analysis of the
477 estimation of the volume of the entire orchard. Thus, one of the main advantages of using the
478 implemented methods for characterizing canopy volumes of orchards is the fact that it is no
479 longer needed to sense both sides of rows, as shown in Fig. 5, in which the vehicle first acquired
480 information from the right side of the row and then from the left side.

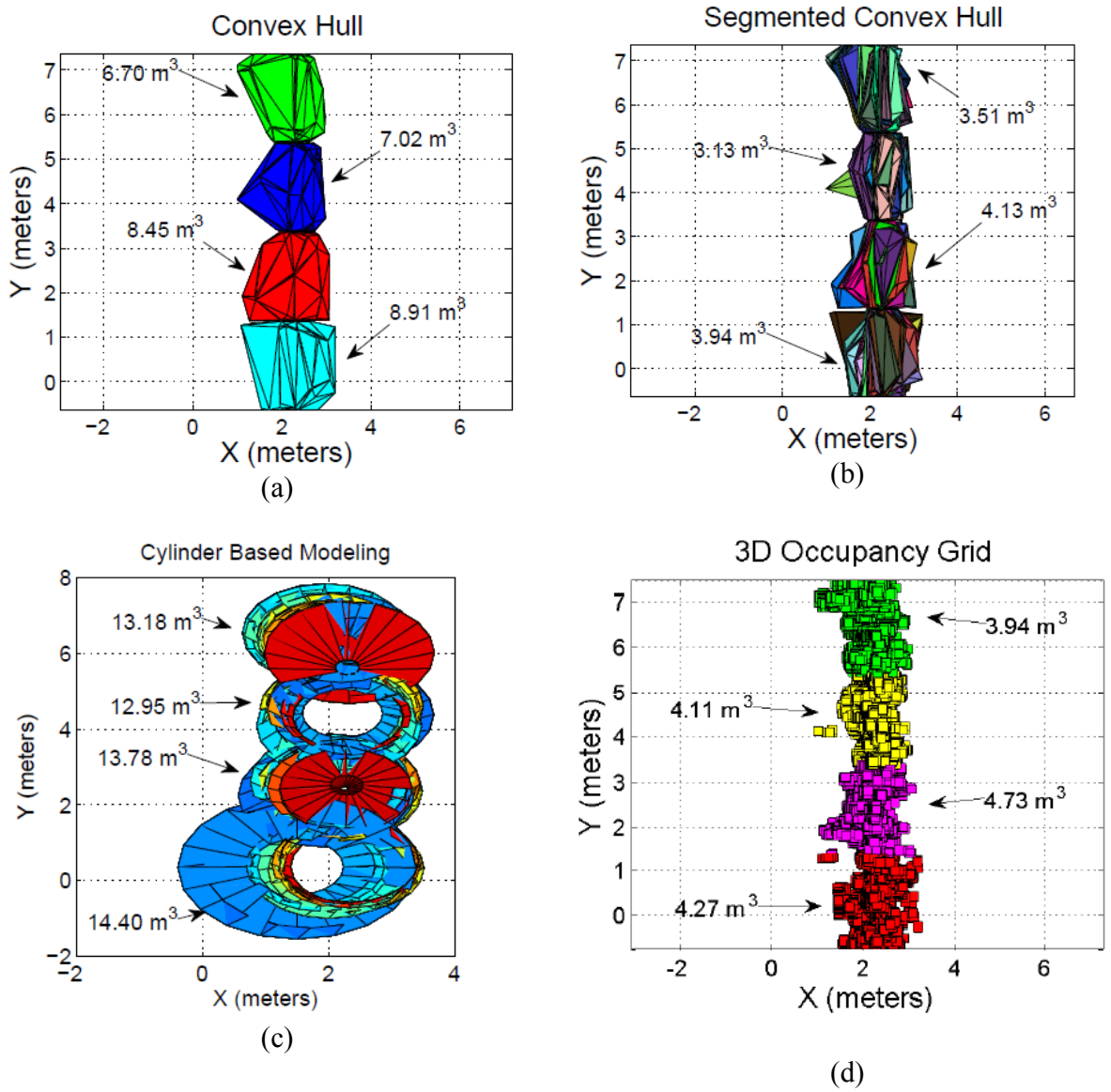

Figure 13- Canopy volume estimation results with partial 3D data batches. Figures 13.a-13.d show the volume estimation for the convex hull, segmented convex hull, cylinder based modeling and 3D occupancy grid approaches, respectively.

Table 1-Comparative analysis of treetop volume estimation between fully and partially scanned orchards.

	Fully scanned canopies (average, m^3)	Partially scanned canopies (average, m^3) (left – right side)	Average estimation correspondence (%)
Convex Hull	36.94	31.08 – 32.03	84
Segmented Convex Hull	21.29	14.71 – 13.97	69
Cylinder-based modeling	62.27	54.31 – 55.18	87
3D occupancy grid	25.06	17.05 – 17.12	68

488

489

490 In Table 1, the third column corresponds to the partially scanned canopies from both right and
491 left LiDAR readings (from the alley-way point of view). The fourth column represents the
492 average estimation correspondence (between the left side and right side LiDAR readings and the
493 fully scanned canopies). As it can be seen both 3D occupancy grid modeling and the segmented
494 convex hull approaches offer the worst volume estimation for partially observable treetops
495 according to the percentual evaluation, since, in both cases, the approaches are able to determine
496 only the 69% (approximately) of the volume obtained with the full data set. It is worth
497 mentioning that if we double the partial volume estimation (for example, for the segmented
498 convex hull approach, if the partial estimation is 14.71 m^3 and we double it for an estimation of
499 the volume of the orchard), then we have overestimated the volume in approximately 38%,
500 which is consistently worse than the previous estimation. As expected, cylinder-based modeling
501 and the convex hull approach show the best volume estimation for partially scanned rows.

Nevertheless, these approaches present the main drawback that any point far from the cluster will drastically increase the estimated volume. The latter can be further improved using filtering techniques to discard outliers.

3.3 Lessons Learned

During the implementation and validation of the proposed techniques, a number of lessons were learned.

1. 3D occupancy grid is the method that performs the best estimate of the treetop volume when the point cloud has a high number of points. Segmented convex hull also leads to good estimates of the volumes.
2. If the efficiency of computing is a priority, the cylinder-based model method followed by the convex hull one are the fastest methods, especially when a small percentage of points is used. However, when the calculations use between 80% and 100% of the data, the relative differences in computing time between the four methods are significantly reduced.
3. When comparing the four methods analyzed it is shown that their behavior with respect to the accuracy and computational cost have opposing trends. Thus, increasing the accuracy also increases the cost of computing, i.e. the most accurate methods are less efficient from the standpoint of computational efficiency.
4. By contrast, large differences between the four methods studied in relation to gradients of the treetop volume estimation, especially starting to 40% of analyzed points are not appreciated.

5. A major drawback of the method of the cylinder-based model is that the existence of isolated points on the periphery of plants causes an exaggerated and unrealistic increase in calculated volume.
6. For partially scanned orchards, when using convex approaches (such as convex-hull or cylinder-based one), choosing the center of mass of segmented points cloud might lead to bias in the volume estimation (as stated in Calders et al. (2013) and Widlowski et al. (2014)). The latter is motivated by the fact that the center of mass is considered the geometric point through where a vertical axis passes (as can be seen in Sections 3.1.2 and 3.1.3). Such center of mass considers all acquired points and no filter or a priori information (such attenuation or penetration of the laser beam) is applied beforehand. Future studies of the authors will be focus on how to minimize such bias in the geometric characterization process.
7. The methods proposed allow to evaluate the volumes from point clouds obtained only from one side of the rows, allowing to simplify the process and reduce the computation time. This may facilitate their possible use in real-time applications.
8. The volume obtained from one side is, in all cases, lower than that obtained considering both sides. If we take as the best estimate of the actual volume of trees the one determined by the 3D occupancy grid method (in this work, 25.06 m^3) then the methods that lead to a better estimate of the volume when applied from a single side are the convex hull and the cylinder-based approaches.
9. The methodological approach used in this work -to assess firstly the different methods with a single object with known geometry and volume, and then apply them to a real case- has proved to be appropriate and effective.

548 10. The four methods tested in this work use only LiDAR range readings. They do not take
549 into account either multi-echo lectures or intensity values since the sensor used is no
550 providing these information in a full wave returned signal. Both LiDAR capabilities
551 could lead to a better estimation of the orchard volume for both partially and fully
552 scanned cases, since information regarding penetration of the beam and its attenuation
553 would be available. The latter is also the focus of the authors' future work.
554
555 **4. Conclusions**
556
557 In this work we have presented, implemented and experimentally validated four methodologies
558 for characterization of canopies. The later was accomplished using 3D LiDAR readings. In
559 particular, two problems were faced: the characterization of fully and partially scanned canopies,
560 with the aim at finding the more appropriate methodology using as metrics the computational
561 cost and the accuracy of the process. The four methods consisted of: a convex hull approach, a
562 segmented convex hull approach, a cylinder-based approach and a 3D grid based approach. The
563 pros and cons of each approach were also included in this work, showing that the cylinder-based
564 and the segmented convex hull approach offered better results when inferring the full
565 characterization of the tree crown based on partial scanning. Thus, the partial knowledge of the
566 crown could lead to a more efficient management of the service unit's resources (e.g., it would
567 not need to traverse all alley-ways in the grove). On the other hand, the 3D grid based approach
568 showed the best tree crown characterization when fully scanned.
569
570

571

572 **Acknowledgments**

573

574 The authors would like to thank to CONICYT (Chile), FONDECYT Grant 1140575, and Basal
575 Grant FB0008. Also, this research was partially funded by the Spanish Ministry of Science and
576 Innovation and by the European Union through the FEDER funds (projects Optidosa-AGL2007-
577 66093-C04-03 and Safespray-AGL2010-22304-C04-03).

578

579 **References**

580 Arnó, J., Escolà, A., Vallès, J.M., Llorens, J., Sanz, R., Masip, J., Palacín, J., Rosell, J.R., 2013.
581 Leaf area index estimation in vineyards using a ground-based LiDAR scanner. Precis. Agric. 14,
582 290-306.

583

584 Arnó, J., Escolà, A., Masip, J., Rosell-Polo, J.R., 2015. Influence of the scanned side of the row
585 in terrestrial laser sensor applications in vineyards: practical consequences. Precis. Agric. 16,
586 119-128.

587

588 Auat Cheein, F., Steiner, G., Perez Paina, G., Carelli, R., 2011. Optimized EIF-SLAM algorithm
589 for precision agriculture mapping based on stems detection. Comput. Electron. Agr. 78, 195-207.

590

591 Auat Cheein, F., Guivant, J., 2014. SLAM-based incremental convex hull processing approach
592 for treetop volume estimation. Computers and Electronics in Agriculture, vol. 102, pp. 19-30.

593

Beland, M., Widlowski, J., Fournier, R., Cote, J., Verstraete, M. 2011. Estimating leaf area distribution in savanna trees from terrestrial LiDAR measurements. Agricultural and Forest Meteorology, 151(9), 1252-1266.

Bucksch, A., Fleck, S., 2009. Automated detection of branch dimensions in woody skeletons of leafless fruit tree canopies. SilviLaser 2009 proceedings, pp. 14-16, Oct. 2009, Austin, Texas.

Bucksch, A., Fleck, S., 2011. Automated detection of branch dimensions in woody skeletons of fruit tree canopies. Photogramm. Eng. Rem. S. 77(3), 229-240.

Calders, K., Lewis, P., Disney, M., Verbesselt, J., Herld, M. 2013. Investigating assumptions of crown archetypes for modeling LiDAR returns, Remote Sensing of Environment, 134, 39-49.

Choset, H., Hutchinson, S., Kantor, G., 2005. Principles of Robot Motion: Theory, Algorithms, and Implementations. MIT Press.

Cote, J., Midlowski, J., Fournier, R. Verstraete, M. 2009. The structural and radiative consistency of three-dimensional tree reconstructions from terrestrial LiDAR. Remote Sensing of Environment, 113, 1067-1081.

Fieber, K., Davenport, I., Ferryman, J., Gurney, R., Walker, J., Hacker, J., 2013. Analysis of full-waveform LiDAR data for classification of an orange orchard scene. ISPRS J. Photogramm. 82, 63-82.

Hosoi, F., Omasa, K. 2006. Voxel-based 3D modeling of individual trees for estimating leaf area density using high-resolution portable scanning LiDAR. IEEE Trans. on Geoscience and Remote Sensing, 44, 3610-3618.

Jaeger-Hansen, C., Griepentrog, H., Andersen, J., 2012. Navigation and Tree Mapping in Orchards. International Conference on Agricultural Engineering, pp. 1-6.

Keightley, K., Bawden, G., 2010. 3D volumetric modeling of grapevine biomass using Tripod LiDAR. Comput. Electron. Agr. 74, 305-312.

Lee, K.H., Ehsani, R., 2009. A laser scanner based measurement system for quantification of citrus tree geometric characteristics. Appl. Eng. Agric. 25 (5), 777–788.

Mella, A., Reina, G., Underwood, J., 2014. A Self-learning Framework for Statistical Ground Classification using Radar and Monocular Vision. J. Field Robot. 32 (1), 20-41.

Méndez, V., Catalán, H., Rosell-Polo, J., Arnó, J., Sanza, R., 2013. LiDAR simulation in modelled orchards to optimise the use of terrestrial laser scanners and derived vegetative measures. Biosystems Eng. 115, 7-19.

638 Méndez, V., Rosell-Polo, J., Sanz, R., Escola, A., Catalán, H., 2014. Deciduous tree
639 reconstruction algorithm based on cylinder fitting from mobile terrestrial laser scanned point
640 clouds. Biosystems Eng. 124, 78-88.
641
642 Moorthy, I., Miller, J., Hu, B., Jimenez, J., Zarco-Tejada, P., Li, Q., 2007. Extracting tree Crown
643 properties from ground-based scanning laser data. IEEE Int. Geoscience and Remote Sensing
644 symposium, pp. 2830-2832, July 2007, Bacelona, Spain.
645
646 Newnham, G., Goodwin, N., Armston, J., Muir, J., Culvenor, D. Comparing time-of-flight and
647 phase-shift terrestrial laser scanners for characterizing topography and vegetation density in a
648 forest environment. SilviLaser 2012, pp. 1-6, September 2012, Vancouver, Canada.
649
650 Pascual, M., Villar, J.M., Rufat, J. Rosell, J.R. Sanz, R., Arnó, J., 2011. Evaluation of peach tree
651 growth characteristics under different irrigation strategies by LIDAR system: preliminary results.
652 Acta Hort. (ISHS). 889, 227-232.
653
654 Pforte, F., Selbeck, J., Hensel, O., 2012. Comparison of two different measurement techniques
655 for automated determination of plum tree canopy cover. Biosystems Eng. 113, 325-333.
656
657 Raumonen, P., Kaasalainen, M., Akerblom, M., Kaasalainen, S., Kaartinen, H., Vastaranta, M.,
658 Holopainen, M., Disney, M., Lewis, P. , 2013. Fast automatic precisión tree models from
659 terrestrial laser scanner data. Remote Sensing, *5*(2), 491-520
660

661 Rosell-Polo, J.R., Sanz, R., Llorens, J., Arnó, J., Escolà, A., Ribes-Dasi, M., Masip, J. Camp, F.,
662 Gràcia, F., Solanelles, F., Pallejà, T., Val, L., Planas, S., Gil, E., Palacín, J., 2009a. A tractor-
663 mounted scanning LIDAR for the non-destructive measurement of vegetative volume and
664 surface area of tree-row plantations: a comparison with conventional destructive measurements
665 Biosystems Eng. 102(2), 128-134.
666
667 Rosell, J.R., Llorens, J., Sanz, R., Arnó, J., Ribes-Dasi, M., Masip, J., Escolà, A., Camp, F.,
668 Solanelles, F., Gràcia, F., Gil, E., Val, L., Planas, S., Palacín, J., 2009b. Obtaining the three-
669 dimensional structure of tree orchards from remote 2D terrestrial LIDAR scanning
670 Agric. For. Meteorol. 149(9), 1505-1515.
671
672 Rosell, J.R., Sanz, R., 2012. A review of methods and applications of the geometric
673 characterization of tree crops in agricultural activities. Comput. Electron. Agr. 81, 124-141.
674
675 Sanz, R., Llorens, J., Escolà, A., Arnó, J., Ribes, M., Masip, J., Camp, F., Gràcia, F., Solanelles,
676 F., Planas, S., Pallejà, T., Palacín, J., Gregorio, E., Del-Moral, I., Rosell, J.R., 2011. Innovative
677 LIDAR 3D dynamic measurement system to estímate fruit-tree leaf area. Sensors, 11(6), 5769-
678 5791.
679
680 Sanz, R., Rosell, J.R., Llorens, J., Gil, E., Planas, S., 2013. Relationship between tree row
681 LIDAR-volume and leaf area density for fruit orchards and vineyards obtained with a LIDAR 3D
682 Dynamic Measurement System. Agricultural and Forest Meteorology, 171/172, 153-162.
683

Walklate, P, Cross, J., Richardson, G., Murray, R., Baker, D., 2002. Comparison of Different Spray Volume Deposition Models using LiDAR Measurements of Apple Orchards. Biosystems Eng. 82, 253-267.

Widlowski, J., Cote, J., Beland, M. 2014. Abstract tree crowns in 3D radiative transfer models: Impact on simulated open-canopy reflectances. Remote Sensing of Environment, 142, 155-175.

Zhang, J., Chambers, A., Maeta, S., Bergerman, M., Singh, S., 2013. 3D Perception for Accurate Row Following: Methodology and Results. IEEE International Conference on Intelligent Robots and Systems, pp. 5306-5313, Nov. 3-7, Tokyo, Japan.

Zhang, J., Maeta, S., Bergerman, M., Singh, S., 2014. Mapping Orchards for Autonomous Navigation, CSBE/ASABE Annual International Meeting, pp. 1-8, July 13-16, Montreal, Canada.

706

707

708

709 **Tables**

710

711 **Table 1**-Comparative analysis of treetop volume estimation between fully and partially scanned

712 orchards.

713

	Fully scanned canopies (average, m^3)	Partially scanned canopies (average, m^3) (left – right side)	Average estimation correspondence (%)
Convex Hull	36.94	31.08 – 32.03	84
Segmented Convex Hull	21.29	14.71 – 13.97	69
Cylinder-based modeling	62.27	54.31 – 55.18	87
3D occupancy grid	25.06	17.05 – 17.12	68

714

715

716

717

718 **Figure Legends**

719

720 **Figure 1-** Non-convex point cloud template. Figure 1.a shows the rigid body used as a template
721 for testing the proposed methodologies for orchard characterization, whereas Fig. 1.b shows the
722 points cloud with 10000 points, belonging to the rigid body.

723

724 **Figure 2-** Experimental olive grove.

725

726 **Figure 3-** Two views of the developed scanning system based on the SICK LiDAR.

727

728 **Figure 4-** Reconstruction of the 3D point cloud obtained with the scanning system shown in Fig.
729 3.

730

731 **Figure 5-** Navigation of the scanning system through the orchard.

732

733 **Figure 6-** Convex hull examples. Figure 6.a shows a point cloud with N = 100 (number of
734 points) according to the template shown in Fig. 1, whereas Fig. 6.b, shows its corresponding
735 convex-hull. Figures 6.c-6.e show the point clouds for N = 1000 and N = 10000, with their
736 corresponding convex-hull (Figs. 6.d-6.f).

737

738 **Figure 7-** Segmented convex hull approach. Figure 7.a shows the case for N = 100, whereas
739 Figs. 7.b and 7.c, show the results for N = 1000 and N = 10000 respectively.

740

741 **Figure 8-** Cylinder-based modeling. Figure 8.a shows the case for N = 100, whereas Figs. 8.b
742 and 8.c show the case for N = 1000 and N = 10000 respectively.
743
744 **Figure 9-** 3D occupancy grid with different size of cells. Figure 9.a shows the case for cells with
745 $\delta = 0.2$ meters of edge's length; whereas Fig. 9.b shows the case for $\delta = 0.4$ meters.
746
747 **Figure 10-** Occupancy grids for different number of points. Figure 10.a shows the case when N
748 = 100; Fig. 10.b shows the case for N = 1000 and Fig. 10.c for N = 10000. The size of cubes
749 remains the same ($\delta = 0.2$ meters).
750
751 **Figure 11-** Performance analysis of the four treetop volume estimation approaches. Figure 11.a
752 shows the behavior of the estimation as function of the number of points in the point cloud
753 associated with the template; Fig. 11.b shows the computational cost (in seconds) of each
754 approach according to the number of points of the cloud; and Fig. 11.c, shows the gradient
755 behavior (obtained from Fig. 11.a).
756
757 **Figure 12-** Volume estimation of a fully observed canopy. Figures 12.a-12.d show the four
758 methodologies for estimating the row section canopy volume shown in Fig. 4.
759
760 **Figure 13-** Canopy volume estimation results with partial 3D data batches. Figures 13.a-13.d
761 show the volume estimation for the convex hull, segmented convex hull, cylinder based
762 modeling and 3D occupancy grid approaches, respectively.